Journal of
Composites Science

MDPI

Article

Design, Preparation, and Characterization of Polycaprolactone–Chitosan Nanofibers via Electrospinning Techniques for Efficient Methylene Blue Removal from Aqueous Solutions

Hind M. Saleh [1], Salim Albukhaty [1,2,*], Ghassan M. Sulaiman [3,*] and Mosleh M. Abomughaid [4]

[1] Department of Chemistry, College of Science, University of Misan, Maysan 62001, Iraq; hind1980@uomisan.edu.iq
[2] College of Medicine, University of Warith Al-Anbiyaa, Karbala 56001, Iraq
[3] Division of Biotechnology, Department of Applied Sciences, University of Technology, Baghdad 10066, Iraq
[4] Department of Medical Laboratory Sciences, College of Applied Medical Sciences, University of Bisha, Bisha 67714, Saudi Arabia; moslehali@ub.edu.sa
* Correspondence: albukhaty.salim@uomisan.edu.iq (S.A.); ghassan.m.sulaiman@uotechnology.edu.iq (G.M.S.)

Abstract: The effective removal of organic dyes from aqueous solutions is of paramount importance in addressing environmental pollution challenges. Methylene blue (MB), a prevalent cationic dye in various industries, has raised concerns due to its persistence and potential adverse effects on ecosystems. This study explores the design, preparation, and characterization of Polycaprolactone–Chitosan (PCL–CH) nanofibers via electrospinning for the removal of MB. PCL, known for its biodegradability and mechanical properties, serves as the primary matrix, while chitosan (CH), with its biocompatibility and amino functionalities, offers enhanced adsorption potential. The electrospinning process yields nanofibers with tailored compositions and controlled morphology. The synthesized nanofibers are systematically characterized, encompassing structural analysis by Fourier transform infrared (FT–IR), spectroscopy, morphology, and composition assessment via Field emission scanning electron microscopy (FE-SEM) and energy-dispersive X-ray spectroscopy (EDS), zeta potential, as well as rheological behavior evaluation. The adsorption uptake of MB onto these nanofibers is investigated, considering the influence of solution pH and initial dye concentration. The results reveal significant enhancements in adsorption capacity, especially with the incorporation of CH, with the PCL–CH 30% nanofibers exhibiting outstanding performance. The pH-dependent behavior underscores the importance of environmental factors in the adsorption process, while higher dye concentrations provide a stronger driving force for adsorption. These findings position PCL–CH nanofibers as promising adsorbents for the efficient removal of MB and potentially other organic contaminants from aqueous solutions. The study contributes to the development of sustainable materials for environmental remediation, wastewater treatment, and related applications, aligning with ongoing efforts to address water pollution challenges.

Keywords: chitosan; electrospinning; methylene blue dye; nanofibers; polycaprolactone

Citation: Saleh, H.M.; Albukhaty, S.; Sulaiman, G.M.; Abomughaid, M.M. Design, Preparation, and Characterization of Polycaprolactone–Chitosan Nanofibers via Electrospinning Techniques for Efficient Methylene Blue Removal from Aqueous Solutions. *J. Compos. Sci.* **2024**, *8*, 68. https://doi.org/10.3390/jcs8020068

Academic Editors: Francesco Tornabene, Thanh Tin Nguyen, Naixin Wang and Duc Viet Nguyen

Received: 10 November 2023
Revised: 31 January 2024
Accepted: 7 February 2024
Published: 9 February 2024

1. Introduction

The growing concern over environmental pollution and the need for sustainable remediation strategies have fueled significant research into innovative materials for the removal of pollutants from aqueous solutions [1]. Among the various classes of contaminants, organic dyes, commonly used in industries such as textiles, printing, and pharmaceuticals, pose a considerable environmental threat due to their persistence and potential toxicity [2]. Methylene blue (MB), a cationic dye widely employed in these industries, has emerged as a prominent target for removal due to its prevalence in wastewater discharges [3]. MB

has been employed in many applications for various industries, including the textile industry where it is commonly used as a dye for cotton, wool, and silk [4]. It is used in the dyeing of garments to give them a blue tint. In medical and biological staining, MB is an important stain for biological specimens in microscopy in the medical industry; MB has historical relevance in photography as a developing agent. It is used for staining tissues and cells, assisting in the visualization of structures [5]. MB finds applications in chemical and pharmaceutical laboratories as an indicator. It is used to determine reducing substances and test for the presence of oxygen [6]. MB is employed as a model dye in studies related to wastewater treatment. Its removal from industrial effluents is a crucial aspect of environmental management [7].

Efforts to combat the environmental impact of such dyes have led to the development of advanced adsorption materials and techniques [8,9]. In this context, nanofibrous materials have garnered significant attention for their unique structural attributes and high surface area-to-volume ratios, rendering them promising candidates for efficient pollutant removal [10,11]. Among these nanofibers, those composed of polycaprolactone (PCL) and chitosan (CH) have exhibited remarkable potential owing to their complementary properties [12,13]. PCL, a biodegradable and biocompatible polymer, possesses excellent mechanical properties and ease of processing, making it an ideal matrix for nanofiber production [14]. CH, derived from chitin, is renowned for its natural abundance, biodegradability, and functional amino groups that enable versatile chemical modifications [15].

Chitosan/graphene composites, arising from the combination of chitosan's unique properties with graphene's enhanced characteristics, have gained prominence. These composites exhibit superior mechanical strength, electrical conductivity, and adsorption capabilities, making them versatile materials for applications in environmental remediation and biomedical fields [16]. Chitosan/silica-composite with a sol-gel method has potential applications in the textile industry [17]. The combination of these two materials, PCL and CH, offers a unique opportunity to engineer nanofibers with enhanced adsorption capabilities [18].

Electrospinning, a versatile and scalable technique, allows for the fabrication of nanofibers with controlled morphology and tailored compositions [19,20]. In this study, we explore the design and preparation of PCL–CH nanofibers through electrospinning strategies for the removal of MB from aqueous solutions. The rational incorporation of CH within the PCL matrix aims to enhance the adsorption capacity of the resulting nanofibers, making them efficient adsorbents for MB and potentially other contaminants. The investigation encompasses a comprehensive characterization of the synthesized nanofibers, including their structural properties, composition, and rheological behavior. Furthermore, the study delves into the adsorption kinetics and equilibrium of MB onto these nanofibers, considering the effects of solution pH and initial dye concentration. Understanding the adsorption mechanisms and performance of these nanofibers is vital for their potential application in wastewater treatment, environmental remediation, and other fields where the removal of organic dyes is paramount.

In summary, this study presents a systematic approach to design, fabricate, and evaluate PCL–CH nanofibers as effective adsorbents for the removal of MB from aqueous solutions. The findings herein provide valuable insights into the development of sustainable materials for tackling water pollution challenges, contributing to the advancement of eco-friendly and efficient remediation strategies.

2. Materials and Methods

2.1. Materials

Polycaprolactone (PCL; 24980-41-4), chitosan (CH; High molecular weight; deacetylation degree exceeded 75%; 9012-76-4), and methylene blue (MB; 122965-43-9) were purchased from Sigma-Aldrich, St Louis, MO, USA (Figure 1). Glacial acetic acid, absolute ethanol (EtOH), and sodium hydroxide (NaOH, $\geq$96%) were purchased from Tamadkala Co.,Tehran, Iran. All chemical solvents and analytical reagents were used as received.

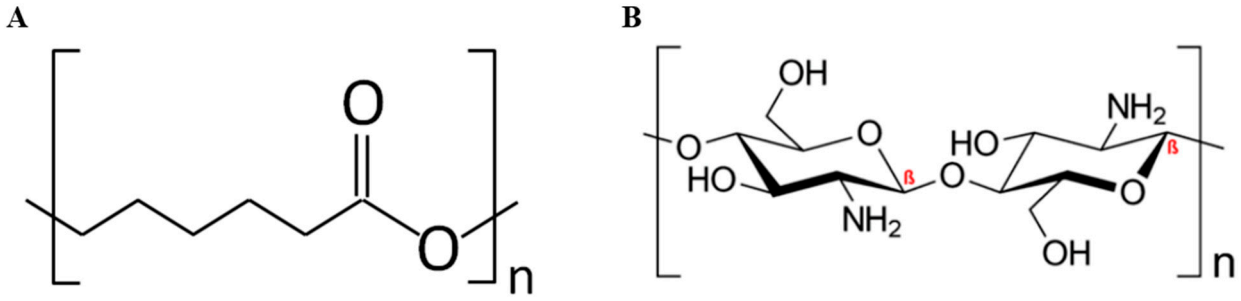

Figure 1. Chemical structures of PCL (**A**) and chitosan (**B**).

2.2. Preparation of PCL–CH Electrospinning Nanofibers

A solution of PCL was prepared by dissolving 20 mg of PCL in 10 mL of glacial acetic acid. The mixture was stirred at room temperature until it achieved homogeneity. In the subsequent step, various amounts of CH (3.50 and 7.00 mg) were dissolved in a mixture of glacial acetic acid and deionized water (in a 70:30 ratio). This solution was also stirred at room temperature for 12 h until it became homogeneous. Finally, both solutions were combined to obtain three different formulations: PCL (without CH), PCL–CH (with 15% *w*/*w* CH), and PCL–CH (with 30% *w*/*w* CH). Each of the PCL–CH solutions (0%, 15%, and 30% CH) was loaded into a 10 mL syringe equipped with a 23 G-sized needle, and the syringe was connected to a syringe pump. A voltage of 27 kV was applied, and the flow rate was maintained at a constant 0.1 mL/h. The distance between the tip of the needle and the collector was set at 21 cm, while the rotating drum's speed was fixed at 100 rpm. With the predetermined voltage, flow rate, tip-to-collector distance, roller speed, and target volume, Taylor's cone was formed, and a polymer jet was successfully generated. It is worth noting that the electromagnetic field influenced the jet's trajectory, causing it to spiral toward the collector. At the collector, a stable polymer jet formed into fibers. These completed nanofibers were carefully peeled from the aluminum foil, washed, and stored for subsequent characterization and dye adsorption studies [21,22].

2.3. Physicochemical Characterization of Nanofibers

The physicochemical properties of nanofibers were characterized by FT-IR, FESEM-EDX, and rheology techniques. The chemical structure and composition of the synthesized nanofibers were assessed using Fourier-transform infrared spectroscopy (FT–IR). Small samples of the nanofibers were carefully prepared and placed on the FT–IR sample holder.

The FT–IR spectra were recorded in the range of 4000–400 cm^{-1} using a high-resolution FT–IR spectrometer [23]. The obtained spectra were analyzed to identify functional groups and chemical bonds within the nanofiber samples. Morphological characteristics and elemental composition of the nanofibers were investigated through field-emission scanning electron microscopy with energy-dispersive X-ray spectroscopy (FESEM–EDX). Thin sections of the nanofiber samples were mounted on FESEM stubs and sputter-coated with a conductive layer. FESEM images were captured under high vacuum conditions, and EDX analysis was performed to identify the elemental composition of the nanofiber samples. The rheological properties of the nanofiber solutions were evaluated using a rheometer. The viscosity and viscoelastic behavior of the PCL–CH solutions (0%, 15%, and 30% CH) were measured at varying shear rates and temperatures [24]. The data obtained from rheological tests were analyzed to understand the flow behavior and viscoelastic characteristics of the solutions, providing insights into their suitability for electrospinning.

2.4. Zeta Potential

Zeta potential analyses of PCL–CH nanofibers were performed using a size analyzer (Malvern Zetasizer Malvern–England) to investigate the surface charge of prepared PCL–CH nanofibers. The electrostatic potential of the fibers was determined using an ultrasonic dispersion of 0.01 g 100 mL^{-1} in DMSO at room temperature.

2.5. Methylene Blue (MB) Adsorption Study

The adsorption capacities of PCL, PCL–CH 15%, and PCL–CH 30% nanofibers for methylene blue (MB) were assessed through batch adsorption experiments. Unless explicitly specified, the MB adsorption experiments were conducted under standardized conditions, with the MB concentration, nanofiber weight, temperature, and pH set at 50 mg/L, 15 mg, 25 °C, and 6, respectively. After the adsorption process, the residual MB concentration in the supernatant solution was quantified using a UV-visible spectrophotometer (UV-2600, Shimadzu, Japan). A calibration curve for MB was established at its maximum wavelength (665 nm). The adsorption capacity (q) and dye removal efficiency (R) of PCL, PCL–CH 15%, and PCL–CH 30% nanofibers were computed using Equations (1) and (2), as follows:

$$q = \frac{(C_0 - C_t)}{m} \times V \quad (1)$$

$$R\% = \frac{(C_0 - C_t)}{C_0} \times 100 \quad (2)$$

where q represents the adsorption capacity (mg/g) of PCL, PCL–CH 15%, and PCL–CH 30% nanofibers. C_0 and C_t are the initial and final concentrations (mg/L) of the MB solution, respectively. V is the volume (L) of the MB solution and m is the weight (g) of the nanofibers.

To investigate the influence of the initial pH of the MB solution on adsorption capacity, 10 mg of nanofiber membrane was immersed in 20 mL of a 50 mg/L MB solution at 25 °C, under varying initial pH conditions ranging from 2 to 10. The residual MB concentration in the supernatant solution was examined after 24 h of adsorption. pH adjustments were made using dropwise additions of 0.1 mol/L NaOH or 0.1 mol/L HCl solution. To study the adsorption isotherms, 15 mg of the nanofiber membrane was immersed in 20 mL of the MB solution at 25 °C with a pH of 6, and varying initial solution concentrations of 25, 50, and 100 mg/L were used. The residual MB concentration in the supernatant solution was assessed after 24 h of adsorption [25].

3. Results and Discussion

3.1. Synthesis and Structural Characterization of PCL–CH Nanofibers

The development of nanofiber materials has gained significant attention in recent years due to their exceptional properties, including high surface area, porosity, and tunable structural characteristics. Electrospinning, as a versatile technique, offers a precise and efficient method for producing nanofibers from various polymer blends. In this context, the preparation of PCL–CH (Polycaprolactone–Chitosan) nanofibers via electrospinning was motivated by several key factors, such as synergistic properties of PCL and CH, enhanced adsorption capability, versatility, customization, and application in MB removal.

3.1.1. FT–IR Spectroscopy Study

The FT–IR spectra are presented in Figure 2A, which shows a comparative analysis of free PCL, free CH, and PCL–CH 30%, serving as a critical step in confirming the successful synthesis of nanofibers. The distinctive transmittance peaks observed in the FT–IR spectrum of PCL are well-documented: the PCL C-O stretching at 726 cm^{-1}, asymmetric stretching of the C-O-C bridge at 1275 cm^{-1}, CH2 deformation at 1452 cm^{-1}, and the presence of carbonyl ester bonds (C=O) at 1730 cm^{-1}. Concurrently, the FT–IR spectrum of CH reveals its characteristic peaks at 1063 cm^{-1}, 1100 cm^{-1}, 1652 cm^{-1}, 2912 cm^{-1}, and 3456 cm^{-1}, corresponding to the C-O stretching, asymmetric stretching of C-O-C bridge, N-H bending, C-H stretching, and O-H stretching, respectively. Intriguingly, the FT–IR spectrum of the nanofiber PCL–CH 15% retains the characteristic peaks of both PCL and CH, albeit with slight shifts.

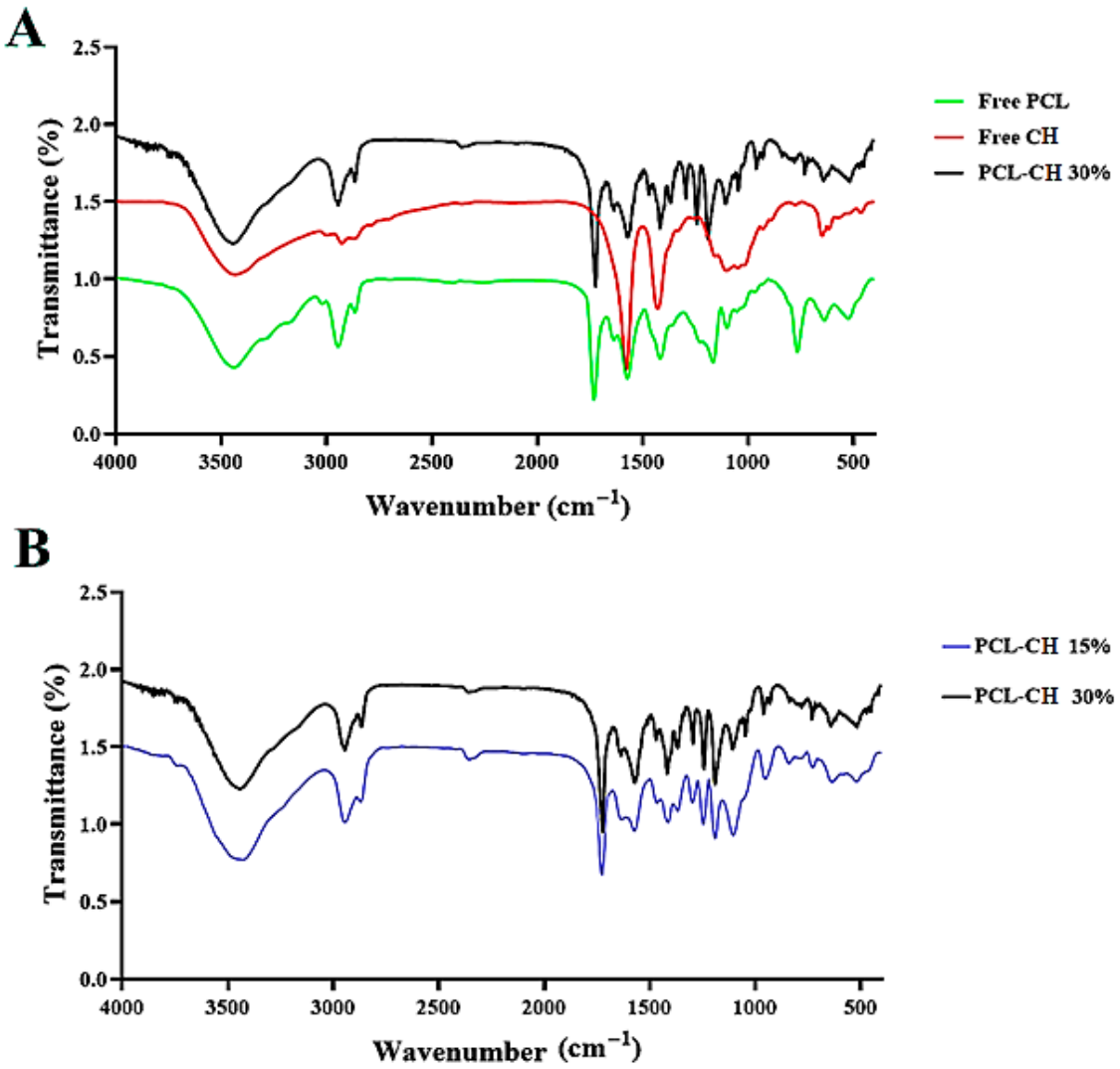

Figure 2. PCL, free CH, and PCL–CH 30% (**A**), and FT–IR spectra of PCL–CH 15% and PCL–CH 30% (**B**).

Additionally, notable peaks at 2900 cm^{-1} and 1600 cm^{-1} are observed, which correspond to the stretching of C-H bonds and the bending of N-H bonds, respectively. The appearance of a peak at 1110 cm^{-1} signifies the presence of the C-O-C bridge (Figure 2B). The FT–IR results offer valuable insights into the structural composition of the synthesized nanofibers. The presence of characteristic peaks from both PCL and CH in the spectrum of PCL–CH 15% indicates the successful integration of these polymers into the nanofiber structure.

The observed shifts in peak positions suggest that bonding intractions between PCL and CH have occurred, resulting in subtle modifications to the chemical environment of the functional groups. These interactions are indicative of molecular compatibility between the two polymers, contributing to the overall stability and cohesiveness of the nanofiber structure. Furthermore, the appearance of distinct peaks associated with C-H and N-H bonds underscores the presence of these groups in the nanofiber composition, corroborating the successful incorporation of CH into the nanofibers [26]. Interestingly, the FT–IR spectra of PCL–CH 15% and PCL–CH 30% demonstrate a consistent spectral pattern, emphasizing the reproducibility and reliability of the electrospinning process in achieving similar compositions for these nanofibers.

3.1.2. FESEM–EDS Analysis

Figure 3A,B presents the FESEM images of the nanofibers, accompanied by their corresponding diameter distribution histograms. All specimens exhibit a uniform and bead-free morphology, indicative of a well-controlled fabrication process. Specifically, the PCL–CH 30% nanofibers exhibit a notably smooth surface, boasting an average diameter of 148.89 ± 9.13 nm. Furthermore, Figure 3C showcases the elemental analysis of the PCL–CH 30% nanofibers, as determined through energy-dispersive X-ray spectroscopy (EDS). The EDS analysis discerns the elemental composition of the nanofibers, providing insights into the primary elements comprising the material. Carbon (C), oxygen (O), and nitrogen (N) are identified as the predominant elements, constituting 72.118%, 2.94%, and 24.88% of the nanofiber composition, respectively. Notably, the PCL–CH 30% nanofibers exhibit a smooth and continuous surface, which is a desirable trait for various applications, including adsorption processes.

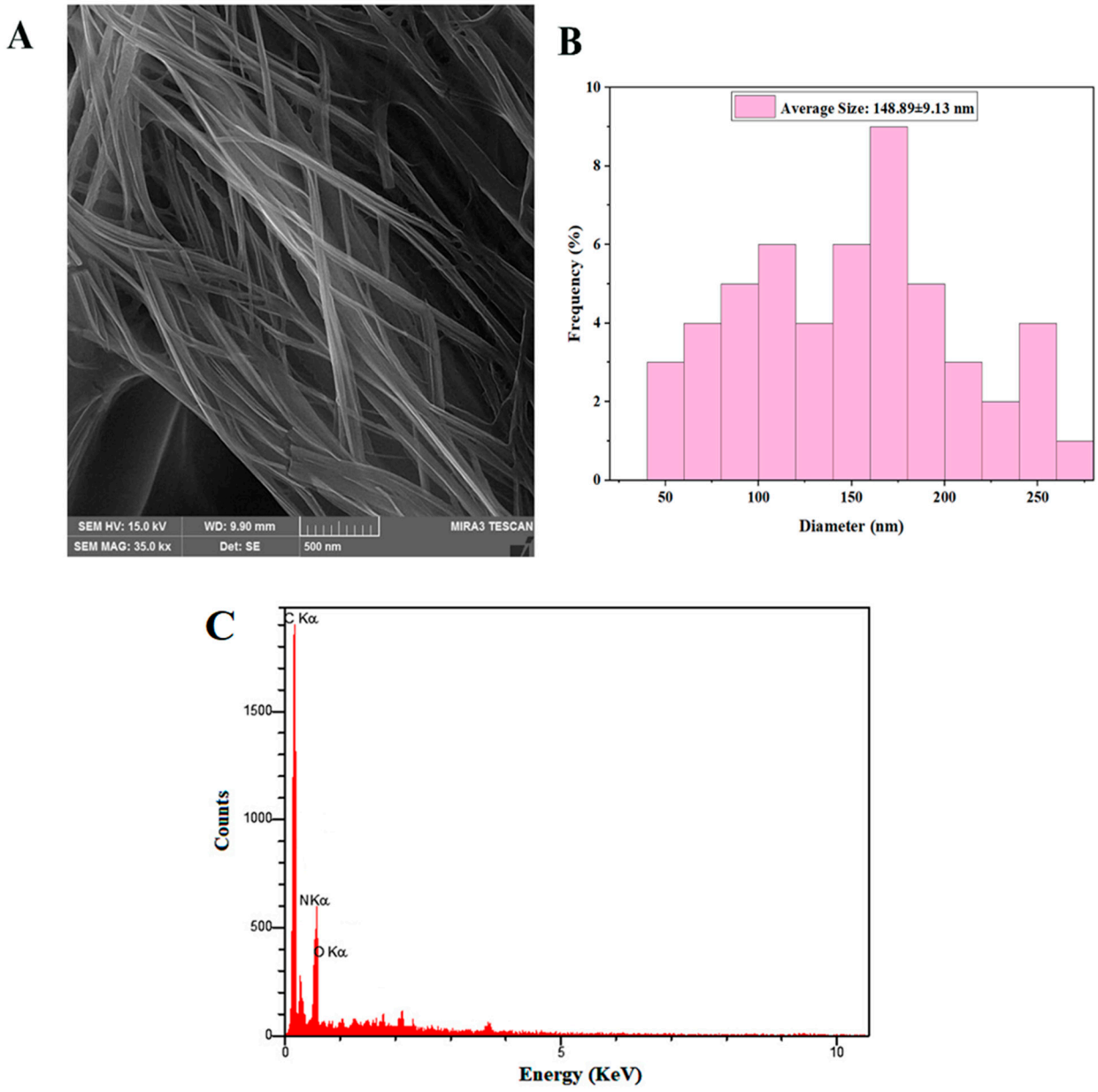

Figure 3. FESEM images of the PCL–CH 30% nanofibers along with histograms of their diameter distributions (**A**,**B**). Energy-dispersive X-ray spectroscopy (EDS) was used to determine the elemental analysis of the PCL–CH 30% nanofibers (**C**).

The observed average diameter of approximately 148.89 nm aligns with the intended nanoscale dimensions, providing a high surface area-to-volume ratio that is advantageous for applications requiring efficient surface interactions. The elemental analysis conducted via EDS serves as a critical characterization tool, elucidating the chemical composition of the PCL–CH 30% nanofibers. The detection of carbon (C), oxygen (O), and nitrogen (N) as the primary elements is consistent with the expected composition based on the constituent polymers, PCL and CH, employed in the fabrication process. These elements are foundational components of organic materials, confirming the organic nature of the nanofibers. The FESEM and EDS results affirm the uniformity and desirable morphology of the nanofibers, specifically highlighting the smooth surface of the PCL–CH 30% nanofibers. The elemental analysis further confirms the anticipated organic composition, and the provided composition percentages offer quantitative data for a comprehensive understanding of the nanofiber material [27,28]. These findings collectively support the suitability of these nanofibers for applications in adsorption processes, including the removal of substances like methylene blue from aqueous solutions.

3.1.3. Zeta Potential Characterization

The surface charge of a material is heavily impacted by electrolytic features (ionic strength, pH level) and material properties (protonation or ionization). The inherent electric charges of the materials utilized in this investigation were determined using a well-established method (Zetasizer) with powdered samples. Figure 4 shows that PCL–CH 30% nanofibers have a zeta potential of 26.4 and remain stable in buffer solutions across all pH ranges.

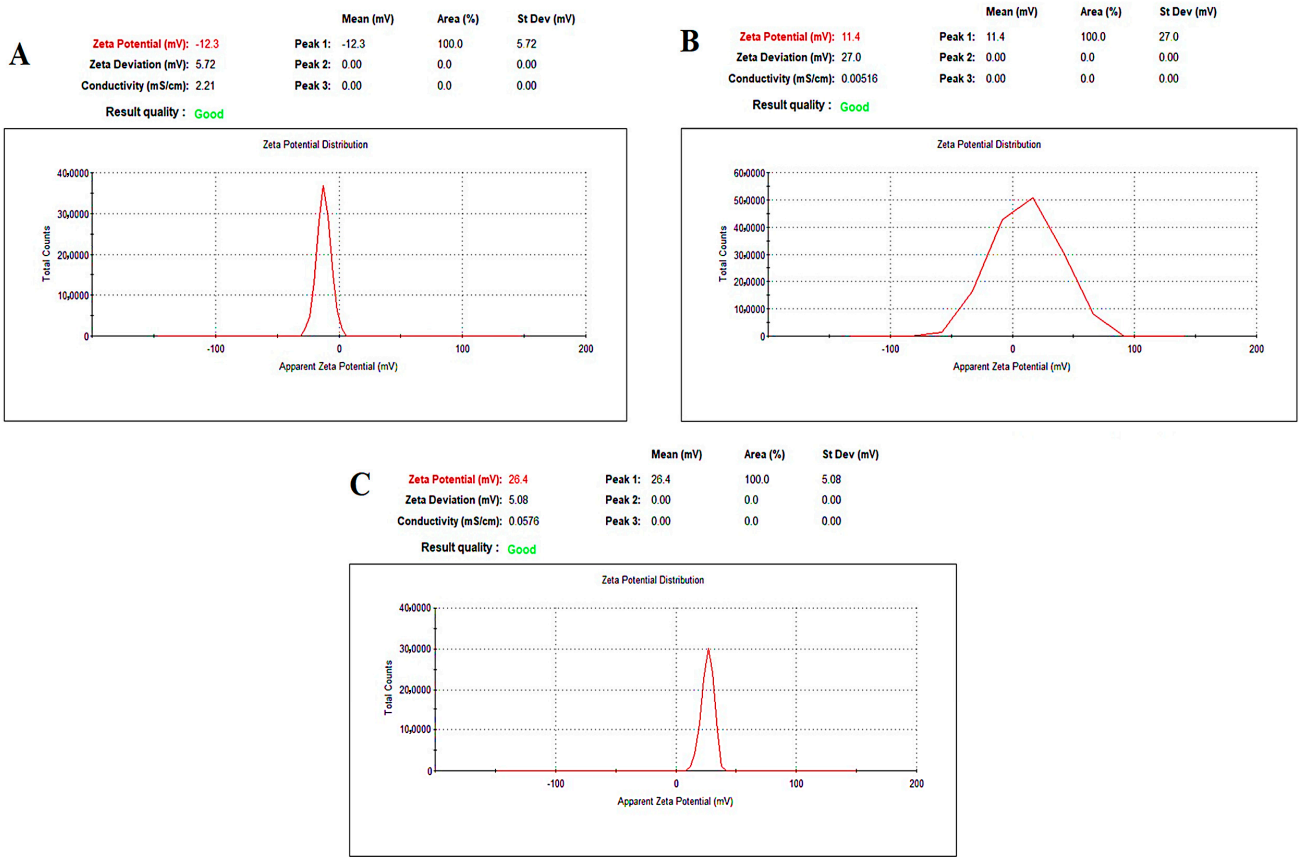

Figure 4. Zeta potentials of PCL–CH nanofibers. (**A**) PCL, (**B**) PCL–CH 15%, and (**C**) PCL–CH 30% nanofibers.

3.1.4. Rheological Behavior Analysis

The rheological behavior of all nanofiber formulations was comprehensively assessed. Figures 5A and 4B present apparent viscosity (Pa) and shear stress (Pas) as functions of shear rate (1/s) for the various nanofibers, including PCL, PCL–CH 15%, and PCL–CH 30%. Figure 5A provides insights into the relationship between shear stress and shear rate across the nanofiber formulations. Notably, for PCL and PCL–CH 15% nanofibers, a discernible decrease in shear stress is observed at lower shear rates (<2 S-1).

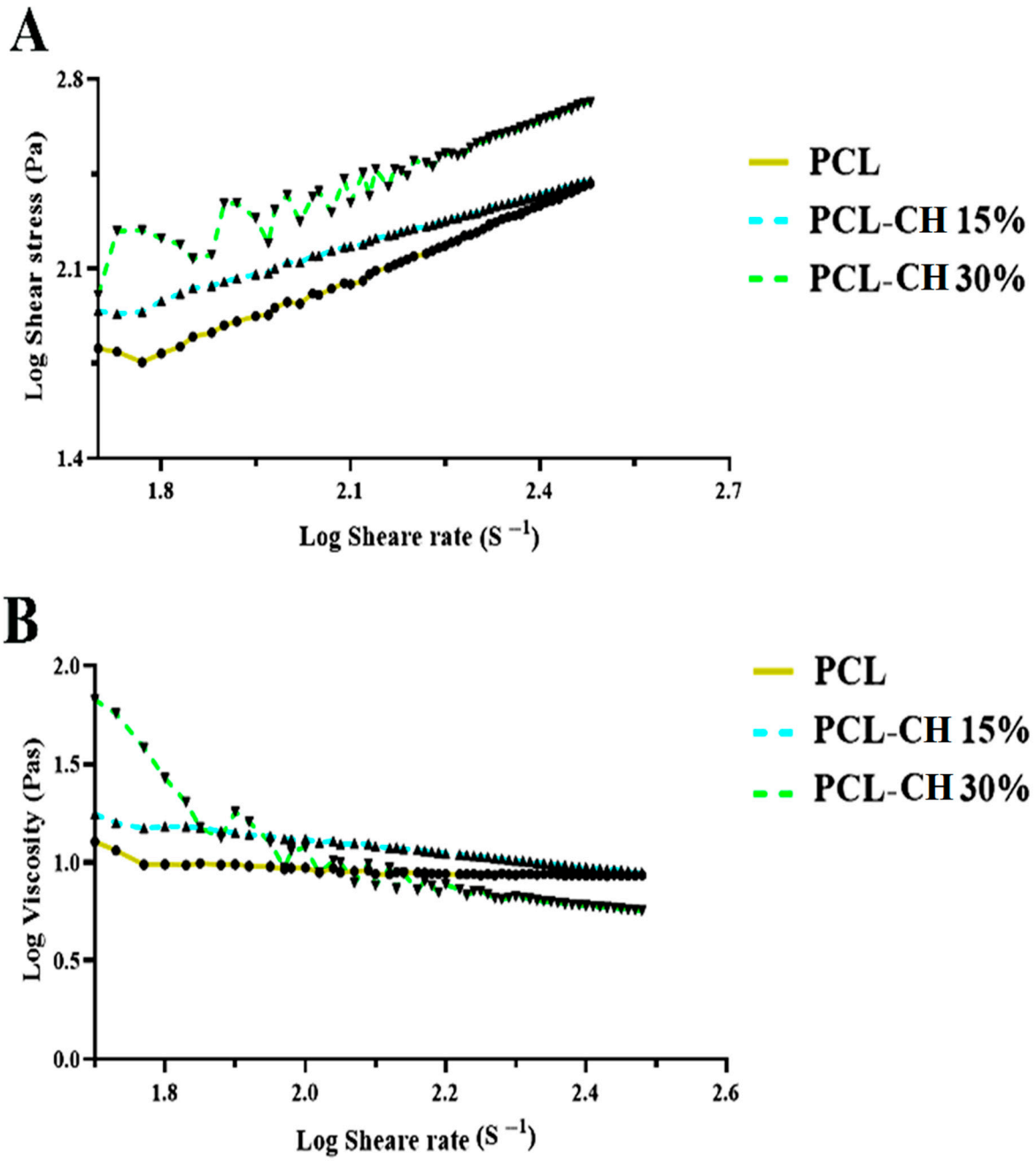

Figure 5. Apparent viscosity (Pa) and shear stress (Pas) as functions of shear rate (1/s) for the various nanofibers, including PCL, PCL–CH 15%, and PCL–CH 30% (**A**,**B**).

In contrast, the PCL–CH 30% nanofiber exhibits somewhat irregular behavior up to a shear rate of 2.2 S-1. However, as the shear rate surpasses 2.2 S-1, a noteworthy and consistent exponential increase in shear stress is witnessed across all nanofiber formulations. This observed behavior is attributed to the distinct characteristics inherent in each nanofiber

formulation. Additionally, Figure 4B illustrates the inverse relationship between viscosity and shear rate for all nanofiber formulations. As the shear rate increases, the viscosity of each formulation decreases proportionally. This dynamic interplay between shear rate and viscosity has implications for the stability and consistency of the nanofibers.

Rheological analysis is instrumental in understanding the flow behavior and viscosity characteristics of nanofiber formulations, providing valuable insights into their applicability for various processes, including electrospinning [29]. The observed decrease in shear stress at lower shear rates (<2 S-1) for PCL and PCL–CH 15% nanofibers is indicative of a pseudoplastic or shear-thinning behavior. This phenomenon signifies that these nanofiber formulations become less viscous and more fluid-like when subjected to lower shear forces, which is advantageous for their processability during electrospinning. In contrast, the somewhat inconsistent behavior of the PCL–CH 30% nanofiber up to 2.2 S-1 suggests the presence of additional factors influencing its rheological response. The exponential increase in shear stress beyond 2.2 S-1 across all nanofiber formulations underscores the influence of nanofiber composition on their flow behavior. This is a crucial finding as it implies that the formulation of nanofibers plays a pivotal role in determining their rheological properties, which can impact their performance in various applications. Furthermore, the decrease in viscosity with increasing shear rate highlights the significance of shear rate on the stability and consistency of the nanofibers. The ability to modulate viscosity under varying shear conditions is advantageous in processes such as electrospinning, where precise control over flow properties is crucial for the formation of uniform and functional nanofibers.

3.2. MB Dye Adsorption Uptake

The adsorption behavior of PCL, PCL–CH 15%, and PCL–CH 30% nanofibers with respect to MB dye over increasing adsorption times is illustrated in Figure 5A. Notably, the adsorption kinetics exhibit distinctive phases characterized by a significant reduction in the adsorption rate during the initial stages, followed by a period of sustained adsorption. This observed trend highlights the influence of MB concentration on the adsorption rate of the adsorbent material. In the early stages of adsorption, higher MB concentrations lead to increased opportunities for contact between MB molecules and the nanofibers. Consequently, this heightened contact results in a more rapid adsorption rate. However, after an adsorption duration of 24 h, a state of saturation is reached, indicating that the MB adsorption process has equilibrated. At this equilibrium point, the adsorption capacities of PCL, PCL–CH 15%, and PCL–CH 30% nanofibers are determined to be 19.33 $\pm$ 3.86 mg/g, 57.92 $\pm$ 3.30 mg/g, and 80.59 $\pm$ 4.60 mg/g, respectively.

The adsorption of MB onto PCL–CH nanofibers is a complex process influenced by the unique properties of both the nanofibers and the dye. The collaboration between chitosan and PCL results in a nanofiber matrix, with improved structural integrity, consistency, and porosity [30,31]. These structural features play a crucial role in providing a stable and accessible surface for MB adsorption, enhancing the overall efficiency of the process. The synergistic combination of chitosan and PCL not only enhances adsorption efficiency but also ensures the stability of the nanofiber structure during the adsorption process [32]. This stability is crucial for maintaining consistent and reliable performance in adsorption studies. The adsorption of MB onto PCL–CH nanofibers involves a combination of hydrogen bonding and the unique surface properties of the nanofibers [33]. Understanding these aspects is crucial for optimizing the design of nanofibers as efficient adsorbents for cationic dyes like MB. This hydrophobic region can interact with the hydrophobic domains of the PCL nanofibers, promoting adsorption, as summarized in Figure 6.

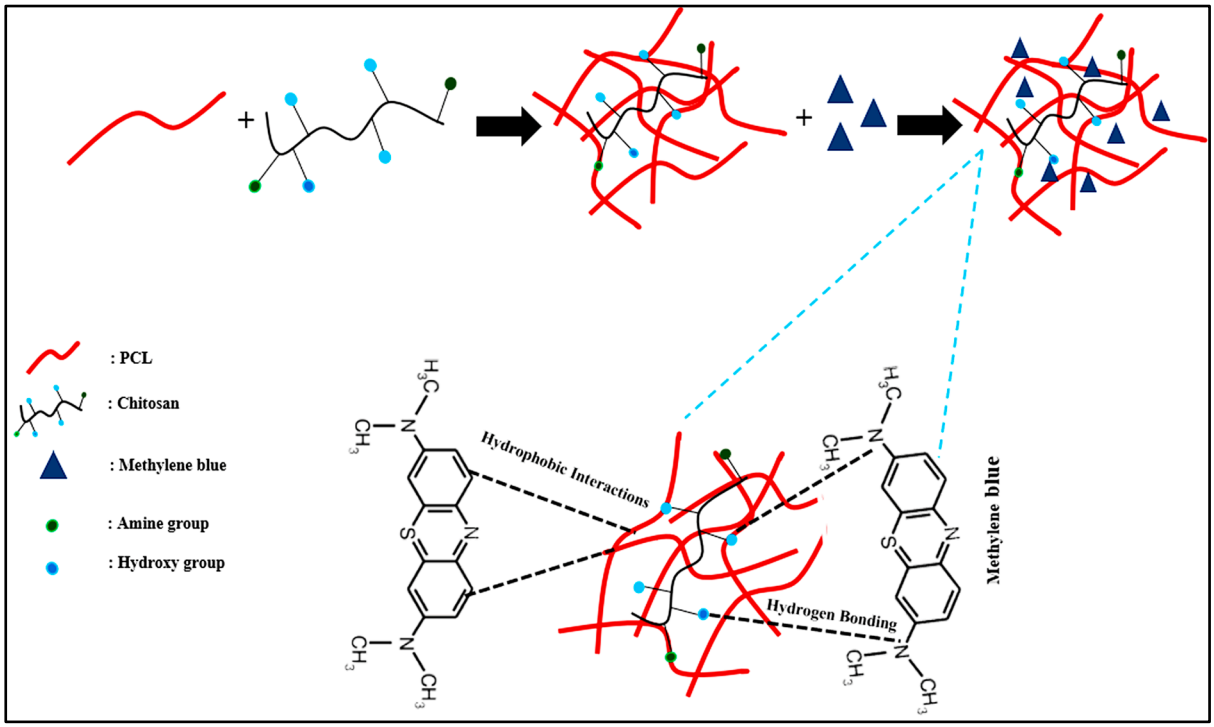

Figure 6. The adsorption mechanism of nanofibers (PCL–CH).

Remarkably, the adsorption capacity of PCL–CH 30% nanofibers surpasses that of PCL by approximately 4.17 times and exceeds that of PCL–CH 15% nanofibers by a factor of 0.72. This substantial difference underscores the significantly enhanced adsorption capability of PCL–CH 30% nanofibers. The pronounced improvement in adsorption performance is attributed to the heightened porosity of PCL–CH 30% nanofibers. Furthermore, it is essential to recognize that adsorption is fundamentally an equilibrium process. Elevated MB concentrations provide a stronger driving force for adsorption, consequently promoting the overall adsorption process.

The adsorption kinetics presented in Figure 7A unveil critical insights into the dynamic interaction between the nanofiber adsorbents and the MB dye. The observed initial reduction in the adsorption rate can be attributed to the limited availability of active adsorption sites on the nanofiber surface. As the adsorption process initiates, these sites become increasingly occupied, leading to a decline in the rate of adsorption. Subsequently, the equilibrium phase is reached after 24 h, marking the point at which the adsorption rate stabilizes. At this juncture, the adsorption capacities of the nanofiber formulations are determined, with PCL–CH 30% nanofibers exhibiting a notably superior adsorption capacity compared to PCL and PCL–CH 15% nanofibers. This substantial enhancement is attributed to the increased porosity of PCL–CH 30% nanofibers, which provides a greater surface area for MB molecules to interact with and be retained [34]. The correlation between MB concentration and the driving force for adsorption is a critical factor to consider. Higher MB concentrations yield a stronger propensity for molecules to adhere to the adsorbent material, thereby enhancing the adsorption process. This principle underscores the importance of tailoring adsorbent materials to the specific adsorption requirements of the target molecules and concentrations, particularly in applications like wastewater treatment and environmental remediation [35]. Experimental data revealed that MB dye uptake was a quick process that achieved equilibrium after about 5 min at pH 10. The equilibrium data were examined using the Langmuir and Freundlich isotherm models [36]. Liang and his colleagues used kinetic, isotherm, and thermodynamic models to explore the adsorption behaviors of MB dye onto nano-carbon composites [37]. The addition of chitosan to polycaprolactone (PCL) nanofibers has been found to have a positive effect

on their mechanical properties. The incorporation of chitosan-assembled graphene oxide (GO–CS) nanohybrid and GO sheets into PCL nanocomposites resulted in an increase in tensile strength and Young's modulus compared to pure PCL [13,38]. Additionally, the inclusion of *Cordia myxa* fruit extract (CMFE) in PCL/chitosan (PCL/CH) nanofibers led to improved physicomechanical and mechanical characteristics [39]. The blend of electrospun chitosan/polycaprolactone (CS/PCL) loaded with *M. communis* leaf extract (MCLE) also enhanced the tensile strength of the nanofiber mats [40]. Furthermore, the incorporation of curcumin (Cur) and zinc oxide nanoparticles (ZnO) in PCL/chitosan (PCL/CS) nanofibers resulted in increased tensile strength and elongation at break [39]. These findings suggest that the addition of chitosan to polycaprolactone nanofibers can improve their mechanical properties, making them suitable for various applications, including wound dressings.

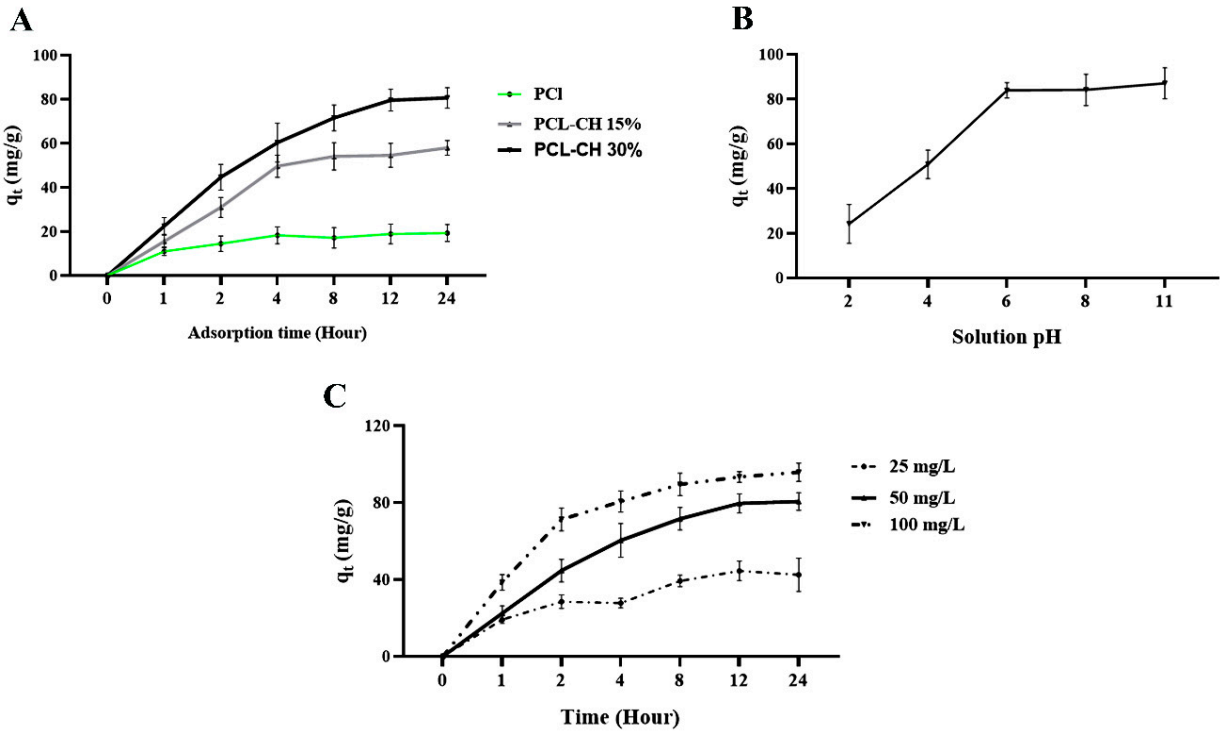

Figure 7. The effects of starting MB adsorption time (**A**), pH (**B**), and initial solution concentration time (**C**) of MB on PCL–CH nanofibers.

The incorporation of chitosan in polycaprolactone (PCL) affects its adsorption capacity. Chitosan has been found to enhance the adsorption capacity of PCL-based materials [41]. A recent study conducted by Martínez and his co-workers indicated that a chitosan-reinforced PCL composite showed adsorption equilibrium capacities for various metal ions, including Zn (II), Cu (II), Fe (II), and Al (III) [42]. Another study investigated the effect of chitosan-assembled graphene oxide (GO–CS) on the microstructure and mechanical properties of PCL nanocomposites [43]. It was observed that the addition of GO–CS nanohybrid and GO sheets increased the tensile strength and Young's modulus of the PCL nanocomposite films [44]. These findings suggest that the incorporation of chitosan in PCL-based materials can improve their adsorption capacity, making them promising materials for water remediation and other applications [41].

The interaction between chitosan and polycaprolactone in fabricated nanofibers plays a crucial role in the observed MB adsorption behavior. While chitosan contains amino ($–NH_2$) and hydroxyl (–OH) groups, it is important to note that in the context of the nanofiber fabrication with PCL, the amino groups may interact with the carbonyl groups (C=O) of PCL through hydrogen bonding. This interaction results from the compatibility of the functional groups in the two polymers. The amino groups of chitosan may form hydrogen bonds with the carbonyl groups of PCL, creating a cohesive and stable nanofiber structure.

This interaction enhances the compatibility of the two polymers during the electrospinning process. The interaction between chitosan and PCL contributes to the overall structural integrity of the nanofibers [18]. This compatibility is essential for creating a uniform and stable nanofiber matrix, which, in turn, influences the adsorption capacity and efficiency of the nanofibers. The interaction between chitosan and PCL, especially through hydrogen bonding, can influence the surface properties and porosity of the nanofibers. These factors play a crucial role in the adsorption of MB, as they affect the accessibility of active sites and the overall adsorption capacity of the nanofibers [24].

3.3. Effects of Original MB Solution pH and Concentration

Figure 7B depicts the impact of the initial pH of the MB solution on the adsorption capacity of the nanofibers. The adsorption capacity of PCL–CH 30% nanofibers experiences a substantial increase with the rising pH of the MB solution, ranging from 24.19 ± 8.68 to 87.03 ± 6.93 mg/g within the pH range of 2 to 10. Notably, the highest MB removal rate, reaching 90.41%, is achieved when the pH of the MB solution is set at 10. This finding underscores the remarkable efficiency of PCL–CH 30% nanofibers as potent adsorbents for MB removal. Furthermore, it reveals that an alkaline environment enhances the adsorption of MB. This phenomenon can be attributed to the pH-dependent behavior of the amino groups present in CH. Under acidic conditions, these amino groups protonate, yielding a positive charge. Consequently, electrostatic repulsion arises between the cationic MB molecules and the positively charged active sites on the adsorbent, resulting in diminished adsorption capacity. In Figure 7C, the effect of the initial concentration of the MB solution on the adsorption capacity of PCL–CH 30% nanofibers is depicted. During the initial stages of adsorption, a high adsorption rate is observed. However, this rate significantly diminishes as the adsorption time progresses, ultimately reaching equilibrium after 24 h. This behavior is attributed to the availability of a substantial number of active adsorption sites on the PCL–CH nanofiber surface at the commencement of adsorption, leading to rapid adsorption. Over time, the occupancy of these active sites by MB molecules increases, giving rise to a strong repulsive force between adsorbed MB ions and unabsorbed ones. Consequently, the remaining sites become progressively more challenging to occupy, ultimately reaching an equilibrium state of adsorption and desorption. Importantly, the equilibrium adsorption capacity of PCL–CH 30% nanofibers displays an increase, corresponding to the elevation of the initial MB solution concentration.

This phenomenon can be attributed to the higher concentration of the initial MB solution, which imparts a greater driving force for breaking through mass transfer resistance. These results collectively emphasize the profound influence of both the initial pH and concentration of the MB solution on the adsorption process [45]. The investigation into the effects of the initial pH and concentration of the MB solution on adsorption yields crucial insights into the performance and mechanisms of the PCL–CH 30% nanofibers as adsorbents. The notable increase in adsorption capacity with rising pH underscores the sensitivity of the adsorption process to the pH environment. The enhanced adsorption at higher pH values is attributed to the deprotonation of amino groups in CH, resulting in negatively charged functional groups. This change facilitates stronger electrostatic interactions with cationic MB molecules, promoting their adsorption onto the positively charged active sites of the nanofibers [46]. In contrast, under acidic conditions, protonation of amino groups reduces electrostatic attraction, leading to reduced adsorption capacity. Regarding the initial concentration of the MB solution, the rapid adsorption rate at the outset is indicative of the availability of numerous active adsorption sites on the nanofiber surface [47,48]. As the adsorption proceeds, these sites become progressively occupied, and the repulsive forces between adsorbed and unabsorbed MB ions hinder further adsorption. Ultimately, equilibrium is attained. The positive correlation between equilibrium adsorption capacity and initial MB solution concentration underscores that a greater driving force is associated with higher concentrations [49,50]. This results in a more efficient breaking of mass transfer resistance barriers, leading to increased adsorption.

3.4. Kinetic Analysis

The pseudo-first-order model and pseudo-second-order model were used to understand the adsorption kinetics, as shown in Figure 8A,B and Table 1. The two adsorption models can be expressed by Equations (3) and (4) [51,52]:

$$\mathrm{Log}(q_e - q_t) = Log\ q_e - K_1 t \quad (3)$$

$$\frac{t}{q_t} = \frac{1}{K_2 q_2^2} + \frac{t}{q_e} \quad (4)$$

where q_e (mg/g) is the amount of adsorbed MB at equilibrium, q_t (mg/g) is the amount of adsorbed MB at time t, and K_1 (min^{-1}) and K_2 (g/mg·min) are the pseudo-first-order rate constant and the pseudo-second-order rate constant, respectively. The pseudo-first-order kinetic model is based on the assumption that the adsorption process is the physical adsorption. The second-order model is based on the assumption that the adsorption process is the chemical adsorption, including the electron sharing and electron transfer between the adsorbent and adsorbate. The kinetic parameters of K_1, K_2, and q_e, as well as the correlation coefficients (R^2), were obtained by linear regression. It can be seen that the theoretical value of the adsorption capacity calculated by the pseudo-second-order model was 101.010 mg/g, which was closer to the experimental value of the adsorption capacity (95.74 mg/g). Moreover, the R^2 (0.989) of the pseudo-second-order model was larger than that of the pseudo-first-order model. Those results indicate that the adsorption process of the PCL–CH nanofiber membrane follow the pseudo-second-order model rather than the pseudo-first-order model

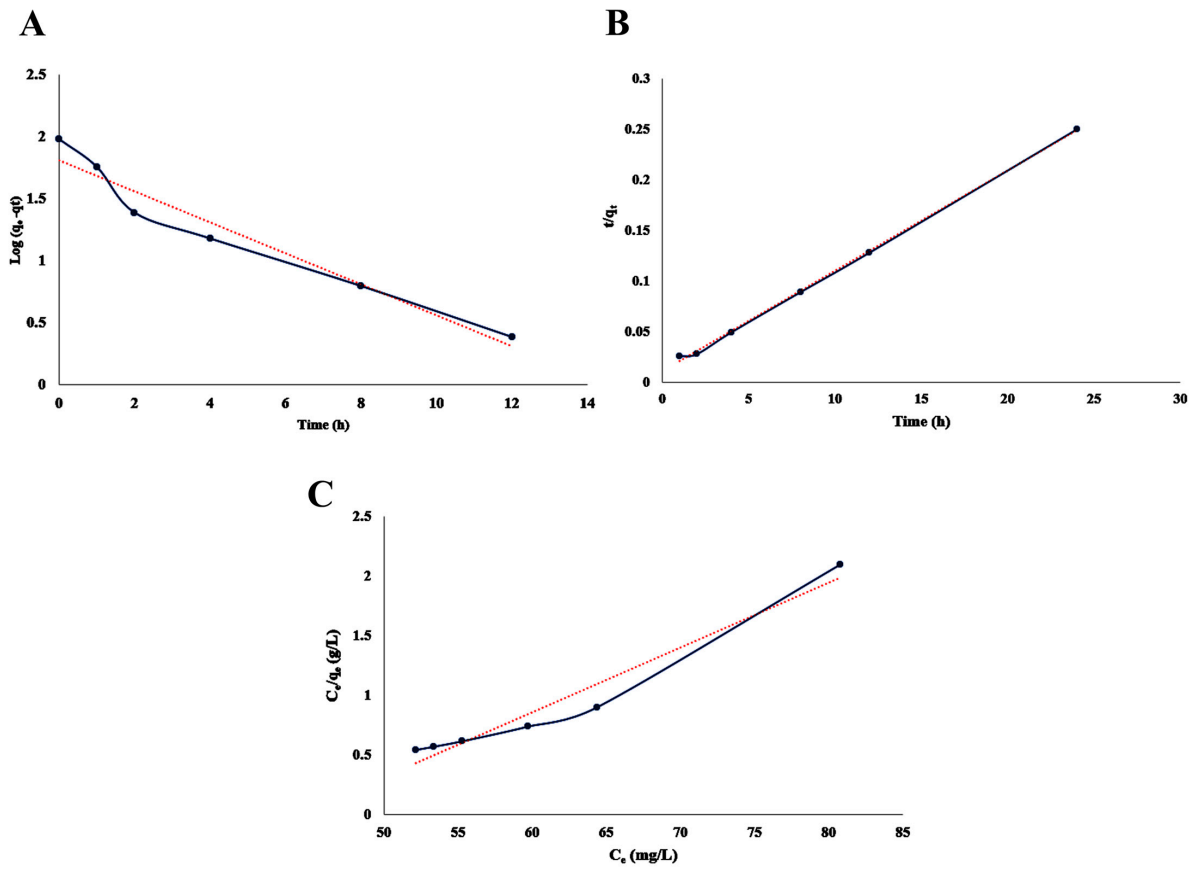

Figure 8. The pseudo-first-order model and pseudo-second-order model were used to understand the adsorption kinetics plots of MB dye adsorption using PCL/CH nanofibers (**A**,**B**), and the adsorption isotherms simulated according to the Langmuir model (**C**). The black line represents the main results while the red line represents the predicted results

Table 1. Kinetic parameters of MB dye adsorption using PCL/CH nanofibers.

Kinetic Analysis				
Model	**Curve Equation**		**Parameters**	
pseudo-first-order	y = −0.1249x + 1.8114	R^2 = 0.9510	K_1 = 0.1249	q_e = 64.774
pseudo-second-order	y = 0.0099x + 0.011	R^2 = 0.9989	K_2 = 0.0089	q_e = 101.010
Adsorption Isotherm				
Langmuir	y = 0.0544 − 2.399	R^2 = 0.9556	K_L = 0.0226	q_m = 18.382

3.5. Adsorption Isotherm

The Langmuir model was applied to study the equilibrium adsorption isotherm of the PCL–CH nanofiber membrane, as shown in Equation (5) [53]:

$$\frac{C_e}{q_e} = \frac{1}{q_0 K_L} + \frac{1}{q_0 C_e} \quad (5)$$

where K_L (L/mg) and q_0 (mg/g) are the Langmuir isothermal constants of the adsorption rate and the adsorption capacity, respectively. For the Langmuir model, it was assumed that the adsorption was localized on a monolayer, and the adsorbent had homogeneous adsorption sites. Adsorption equilibrium is a dynamic process; that is, the adsorption equilibrium was reached when the adsorption rate was equal to the desorption rate. The adsorption isotherms simulated according to the Langmuir model are shown in Figure 7C. The original MB solution pH was 6.5, and the test temperature was 25 °C. The theoretical value of the adsorption capacity q_m calculated by Langmuir is about 18.382 mg/g, and R2 is 0.9556, which confirms that the PCL–CH membrane is a good adsorbent for MB. This result suggests that the Langmuir model is suitable for describing the adsorption behavior of MB by PCL–CH nanofiber membranes.

4. Conclusions

In conclusion, this study elucidates the design, fabrication, and application of Polycaprolactone–Chitosan (PCL–CH) nanofibers as potent adsorbents for the removal of methylene blue (MB) from aqueous solutions. The investigation highlights the pivotal role of nanofiber composition, morphology, and environmental factors in the adsorption process. The synthesized PCL–CH nanofibers, produced through electrospinning, exhibit controlled morphology, tailored compositions, and desirable structural attributes. Systematic characterization validates their suitability for adsorption applications. Adsorption experiments reveal the remarkable adsorption capacity of PCL–CH nanofibers, with the PCL–CH 30% nanofibers demonstrating exceptional performance. The influence of solution pH underscores the importance of environmental conditions, with alkaline pH enhancing adsorption. Moreover, the positive correlation between initial dye concentration and adsorption capacity highlights the significance of a robust driving force for adsorption. The findings emphasize the potential of PCL–CH nanofibers as efficient and sustainable adsorbents for the removal of MB and other organic dyes from aqueous solutions. Their versatile nature positions them for application in diverse fields, including wastewater treatment and environmental remediation. This study contributes to the advancement of eco-friendly and effective solutions for addressing water pollution challenges. The insights gained underscore the significance of material design and environmental conditions in optimizing adsorption processes, offering a promising avenue for sustainable water treatment and pollutant removal.

Author Contributions: Conceptualization, H.M.S. and S.A.; methodology, H.M.S.; software, G.M.S.; validation, H.M.S. and S.A.; formal analysis, G.M.S.; investigation, S.A. and M.M.A.; resources, H.M.S.; data curation, G.M.S.; writing—original draft preparation, H.M.S.; writing—review and editing, S.A., G.M.S. and M.M.A.; visualization, G.M.S.; supervision, S.A.; project administration, S.A.; funding acquisition, H.M.S. All authors have read and agreed to the published version of the manuscript.

Funding: This research received no external funding.

Institutional Review Board Statement: Not applicable.

Informed Consent Statement: Not applicable.

Data Availability Statement: Data are contained within the article.

Acknowledgments: The authors are thankful to the Deanship of Scientific Research at the University of Bisha for supporting this work through the Fast-Track Research Support Program.

Conflicts of Interest: The authors declare no conflicts of interest.

References

1. Prasannamedha, G.; Kumar, P.S. A review on contamination and removal of sulfamethoxazole from aqueous solution using cleaner techniques: Present and future perspective. *J. Clean. Prod.* **2020**, *250*, 119553. [CrossRef]
2. Shanker, U.; Rani, M.; Jassal, V. Degradation of hazardous organic dyes in water by nanomaterials. *Environ. Chem. Lett.* **2017**, *15*, 623–642. [CrossRef]
3. Fito, J.; Abewaa, M.; Mengistu, A.; Angassa, K.; Ambaye, A.D.; Moyo, W.; Nkambule, T. Adsorption of methylene blue from textile industrial wastewater using activated carbon developed from *Rumex abyssinicus* plant. *Sci. Rep.* **2023**, *13*, 5427. [CrossRef]
4. Khan, I.; Saeed, K.; Zekker, I.; Zhang, B.; Hendi, A.H.; Ahmad, A.; Ahmad, S.; Zada, N.; Ahmad, H.; Shah, L.A.; et al. Review on Methylene Blue: Its Properties, Uses, Toxicity and Photodegradation. *Water* **2022**, *14*, 242. [CrossRef]
5. Peng, Y.J.; Chen, C.M.; Li, Y.F.; Guo, Y.T.; Chen, Y.T.; Chao, K.H.; Yang, J.J. Patent blue versus methylene blue and indigo carmine as a better dye for chromodiscography: In vitro staining efficacy and cytotoxicity study using bovine coccygeal intervertebral discs. *Spine J.* **2023**, *23*, 1079–1087. [CrossRef] [PubMed]
6. Wainwright, M.; Crossley, K. Methylene Blue-a therapeutic dye for all seasons? *J. Chemother.* **2002**, *14*, 431–443. [CrossRef]
7. Samsami, S.; Mohamadizaniani, M.; Sarrafzadeh, M.-H.; Rene, E.R.; Firoozbahr, M. Recent Advances in the Treatment of Dye-Containing Wastewater from Textile Industries: Overview and Perspectives. *Process Saf. Environ. Prot.* **2020**, *143*, 138–163. [CrossRef]
8. Pragya, B.; Antara, B.; Chandralekha, N.; Salini, S.; Megha, P.; Sandra, K.; Goutam, M.A.; Ramesh, W.U.; Kaviyarasi, R.; Balachandar, V.; et al. Recent advances in green technology and Industrial Revolution 4.0 for a sustainable future. *Environ. Sci. Pollut. Res. Int.* **2022**, *30*, 124488–124519.
9. Haleem, A.; Shafiq, A.; Chen, S.-Q.; Nazar, M. A Comprehensive Review on Adsorption, Photocatalytic and Chemical Degradation of Dyes and Nitro-Compounds over Different Kinds of Porous and Composite Materials. *Molecules* **2023**, *28*, 1081. [CrossRef]
10. Aldalbahi, A.; El-Naggar, M.E.; El-Newehy, M.H.; Rahaman, M.; Hatshan, M.R.; Khattab, T.A. Effects of Technical Textiles and Synthetic Nanofibers on Environmental Pollution. *Polymers* **2021**, *13*, 155. [CrossRef]
11. Al-Kaabi, W.J.; Albukhaty, S.; Al-Fartosy, A.J.M.; Al-Karagoly, H.K.; Al-Musawi, S.; Sulaiman, G.M.; Dewir, Y.H.; Alwahibi, M.S.; Soliman, D.A. Development of *Inula graveolens* (L.) Plant Extract Electrospun/Polycaprolactone Nanofibers: A Novel Material for Biomedical Application. *Appl. Sci.* **2021**, *11*, 828. [CrossRef]
12. Sogut, E.; Seydim, A.C.; Chiralt, A. Development of chitosan/cycloolefin copolymer and chitosan/polycaprolactone active bilayer films incorporated with grape seed extract and carvacrol. *J. Polym. Res.* **2021**, *28*, 319. [CrossRef]
13. Alyamani, A.A.; Al-Musawi, M.H.; Albukhaty, S.; Sulaiman, G.M.; Ibrahim, K.M.; Ahmed, E.M.; Jabir, M.S.; Al-Karagoly, H.; Aljahmany, A.A.; Mohammed, M.K.A. Electrospun Polycaprolactone/Chitosan Nanofibers Containing *Cordia myxa* Fruit Extract as Potential Biocompatible Antibacterial Wound Dressings. *Molecules* **2023**, *28*, 2501. [CrossRef]
14. Mandal, P.; Shunmugam, R. Polycaprolactone: A biodegradable polymer with its application in the field of self-assembly study. *J. Macromol. Sci. A* **2020**, *58*, 111–129. [CrossRef]
15. Bakshia, P.S.; Selvakumara, D.; Kadirvelub, K.; Kumara, N.S. Chitosan as an environment friendly biomaterial—A review on recent modifications and applications. *Int. J. Biol. Macromol.* **2020**, *150*, 1072–1083. [CrossRef] [PubMed]
16. Alves, D.C.d.S.; Healy, B.; Yu, T.; Breslin, C.B. Graphene-Based Materials Immobilized within Chitosan: Applications as Adsorbents for the Removal of Aquatic Pollutants. *Materials* **2021**, *14*, 3655. [CrossRef] [PubMed]
17. Chen, G.S.; Haase, H.; Mahltig, B. Chitosan-modified silica sol applications for the treatment of textile fabrics: A view on hydrophilic, antistatic and antimicrobial properties. *J. Sol-Gel Sci. Technol.* **2019**, *91*, 461–470. [CrossRef]
18. Ghahremanzadeh, F.; Alihosseini, F.; Semnani, D. Investigation and comparison of new galactosylation methods on PCL/chitosan scaffolds for enhanced liver tissue engineering. *Int. J. Biol. Macromol.* **2021**, *174*, 278–288. [CrossRef]

19. Lugoloobi, I.; Yuanhao, W.; Marriam, I.; Hu, J.; Tebyetekerwa, M.; Ramakrishna, S. Electrospun biomedical nanofibers and their future as intelligent biomaterials. *Curr. Opin. Biomed. Eng.* **2022**, *24*, 100418. [CrossRef]
20. Albukhaty, S.; Al-Karagoly, H.; Allafchian, A.R.; Jalali, S.A.H.; Al-Kelabi, T.; Muhannad, M. Production and characterization of biocompatible nanofibrous scaffolds made of β-sitosterol loaded polyvinyl alcohol/tragacanth gum composites. *Nanotechnology* **2021**, *33*, 085102. [CrossRef]
21. Chauhan, D.; Dwivedi, J.; Sankararamakrishnan, N. Novel chitosan/PVA/zerovalent iron biopolymeric nanofibers with enhanced arsenic removal applications. *Environ. Sci. Pollut. Res.* **2014**, *21*, 9430–9442. [CrossRef] [PubMed]
22. Ghorbani, F.M.; Kaffashi, B.; Shokrollahi, P.; Seyedjafari, E.; Ardeshirylajimi, A. PCL/chitosan/Zn-doped nHA electrospun nanocomposite scaffold promotes adipose derived stem cells adhesion and proliferation. *Carbohydr. Polym.* **2015**, *118*, 133–142. [CrossRef]
23. Al-Musawi, S.; Albukhaty, S.; Al-Karagoly, H.; Sulaiman, G.M.; Alwahibi, M.S.; Dewir, Y.H.; Soliman, D.A.; Rizwana, H. Antibacterial Activity of Honey/Chitosan Nanofibers Loaded with Capsaicin and Gold Nanoparticles for Wound Dressing. *Molecules* **2020**, *25*, 4770. [CrossRef]
24. Khan, G.; Yadav, S.K.; Patel, R.R.; Kumar, N.; Bansal, M.; Mishra, B. Tinidazole functionalized homogeneous electrospun chitosan/poly (ε-caprolactone) hybrid nanofiber membrane: Development, optimization and its clinical implications. *Int. J. Biol. Macromol.* **2017**, *103*, 1311–1326. [CrossRef] [PubMed]
25. Pavan, F.A.; Lima, E.C.; Dias, S.L.P.; Mazzocato, A.C. Methylene blue biosorption from aqueous solutions by yellow passion fruit waste. *J. Hazard. Mater.* **2008**, *150*, 703–712. [CrossRef]
26. Kahdim, Q.S.; Abdelmoula, N.; Al-Karagoly, H.; Albukhaty, S.; Al-Saaidi, J. Fabrication of a Polycaprolactone/Chitosan Nanofibrous Scaffold Loaded with Nigella sativa Extract for Biomedical Applications. *BioTech* **2023**, *12*, 19. [CrossRef]
27. Eichhorn, S.; Dufresne, A.; Aranguren, M.; Marcovich, E.; Capadona, J.; Rowan, S.; Weder, C.; Thielemans, W.; Roman, M.; Renneckar, S.; et al. Review: Current international research into cellulose nanofibres and nanocomposites. *J. Mater. Sci.* **2010**, *45*, 1–33. [CrossRef]
28. Asghari, F.; Rabiei Faradonbeh, D.; Malekshahi, Z.V.; Nekounam, H.; Ghaemi, B.; Yousefpoor, Y.; Ghanbari, H.; Faridi-Majidi, R. Hybrid PCL/Chitosan-PEO Nanofibrous Scaffolds Incorporated with A. Euchroma Extract for Skin Tissue Engineering Application. *Carbohydr. Polym.* **2022**, *278*, 118926. [CrossRef]
29. Miele, D.; Catenacci, L.; Rossi, S.; Sandri, G.; Sorrenti, M.; Terzi, A.; Giannini, C.; Riva, F.; Ferrari, F.; Caramella, C.; et al. Collagen/PCL Nanofibers Electrospun in Green Solvent by DOE Assisted Process. An Insight into Collagen Contribution. *Materials* **2020**, *13*, 4698. [CrossRef]
30. Abasalta, M.; Asefnejad, A.; Khorasani, M.T.; Saadatabadi, A.R. Fabrication of carboxymethyl chitosan/poly(ε-caprolactone)/doxorubicin/nickel ferrite core-shell fibers for controlled release of doxorubicin against breast cancer. *Carbohydr. Polym.* **2021**, *257*, 117631. [CrossRef]
31. Fadaie, M.; Mirzaei, E.; Geramizade, B.; Asvar, Z. Incorporation of nanofibrillated chitosan into electrospun PCL nanofibers makes scaffolds with enhanced mechanical and biological properties. *Carbohydr. Polym.* **2018**, *199*, 628–640. [CrossRef] [PubMed]
32. Aramesh, N.; Bagheri, A.R.; Bilal, M. Chitosan-Based Hybrid Materials for Adsorptive Removal of Dyes and Underlying Interaction Mechanisms. *Int. J. Biol. Macromol.* **2021**, *183*, 399–422. [CrossRef]
33. Zhang, Y.; Wang, F.; Wang, Y. Recent Developments of Electrospun Nanofibrous Materials as Novel Adsorbents for Water Treatment. *Mater. Today Commun.* **2021**, *27*, 102272. [CrossRef]
34. Kozehkonan, G.S.; Salehi, M.; Farzamfar, S.; Ghanbari, H.; Adabi, M.; Amani, A. Preparation and characterization of PCL polymeric scaffolds coated with chitosan/bioactive glass/gelatin nanoparticles using the tips methodology for bone tissue engineering. *Nanomed. J.* **2019**, *6*, 311–320.
35. Agrawal, S.; Ranjan, R.; Lal, B.; Rahman, A.; Singh, S.P.; Selvaratnam, T.; Nawaz, T. Synthesis and Water Treatment Applications of Nanofibers by Electrospinning. *Processes* **2021**, *9*, 1779. [CrossRef]
36. Tang, X.; Ran, G.; Li, J.; Zhang, Z.; Xiang, C. Extremely efficient and rapidly adsorb methylene blue using porous adsorbent prepared from waste paper: Kinetics and equilibrium studies. *J. Hazard. Mater.* **2021**, *402*, 123579. [CrossRef] [PubMed]
37. Liang, C.; Shi, Q.; Feng, J.; Yao, J.; Huang, H.; Xie, X. Adsorption Behaviors of Cationic Methylene Blue and Anionic Reactive Blue 19 Dyes onto Nano-Carbon Adsorbent Carbonized from Small Precursors. *Nanomaterials* **2022**, *12*, 1814. [CrossRef]
38. Shahsavar, F.; Babaei, A. Investigating the effect of chitosan functionalized graphene oxide on the performance of biodegradable polycaprolactone. *J. Reinf. Plast. Compos.* **2023**. [CrossRef]
39. Mosallanezhad, P.; Nazockdast, H.; Ahmadi, Z.; Rostami, A. Fabrication and characterization of polycaprolactone/chitosan nanofibers containing antibacterial agents of curcumin and ZnO nanoparticles for use as wound dressing. *Front. Bioeng. Biotechnol.* **2022**, *10*, 1797. [CrossRef]
40. Modiri-Delshad, T.; Ramazani, A.; Khoobi, M.; Akbari Javar, H.; Akbari, T.; Amin, M. Fabrication of chitosan/polycaprolactone/Myrtus communis L. extract nanofibrous mats with enhanced antibacterial activities. *Polym. Polym. Compos.* **2023**, *31*. [CrossRef]
41. Kayan, G.Ö.; Kayan, A. Polycaprolactone Composites/Blends and Their Applications Especially in Water Treatment. *ChemEngineering* **2023**, *7*, 104. [CrossRef]
42. Martínez, M.E.; Rangel-Méndez, J.R.; Gimeno, M.; Tecante, A.; Lapidus, G.T.; Shirai, K. Removal of Heavy Metal Ions from Wastewater with Poly-ε-Caprolactone-Reinforced Chitosan Composite. *Polymers* **2022**, *14*, 5196. [CrossRef]

43. Wang, C.; Zhang, Z.; Chen, B.; Gu, L.; Li, Y.; Yu, S. Design and evaluation of galactosylated chitosan/graphene oxide nanoparticles as a drug delivery system. *J. Colloid Interface Sci.* **2018**, *516*, 332–341. [CrossRef]
44. Heidari, M.; Bahrami, S.H.; Ranjbar-Mohammadi, M.; Milan, P.B. Smart electrospun nanofibers containing PCL/gelatin/graphene oxide for application in nerve tissue engineering. *Mater. Sci. Eng. C* **2019**, *103*, 109768. [CrossRef]
45. Fu, J.; Chen, Z.; Wang, M.; Liu, S.; Zhang, J.; Zhang, J.; Han, R.; Xu, Q. Adsorption of methylene blue by a high-efficiency adsorbent (polydopamine microspheres): Kinetics, isotherm, thermodynamics and mechanism analysis. *Chem. Eng. J.* **2015**, *259*, 53–61. [CrossRef]
46. Zhang, T.J.; Xiao, S.Y.; Fan, K.H.; He, H.; Qin, Z.Y. Preparation and adsorption properties of green cellulose-based composite aerogel with selective adsorption of methylene blue. *Polymer* **2022**, *258*, 125320. [CrossRef]
47. El-Bery, H.M.; Saleh, M.; El-Gendy, R.A.; Saleh, M.R.; Thabet, S.M. High adsorption capacity of phenol and methylene blue using activated carbon derived from lignocellulosic agriculture wastes. *Sci. Rep.* **2022**, *12*, 5499. [CrossRef]
48. Cheng, J.; Zhan, C.; Wu, J.; Cui, Z.; Si, J.; Wang, Q.; Peng, X.; Turng, L.S. Highly Efficient Removal of Methylene Blue Dye from an Aqueous Solution Using Cellulose Acetate Nanofibrous Membranes Modified by Polydopamine. *ACS Omega* **2020**, *5*, 5389–5400. [CrossRef]
49. Albadarin, A.B.; Collins, M.N.; Naushad, M.; Shirazian, S.; Walker, G.; Mangwandi, C. Activated lignin-chitosan extruded blends for efficient adsorption of methylene blue. *Chem. Eng. J.* **2017**, *307*, 264–272. [CrossRef]
50. Taleb, F.; Ammar, M.; Mosbah, M.B.; Salem, R.B.; Moussaoui, Y. Chemical modification of lignin derived from spent coffee grounds for methylene blue adsorption. *Sci. Rep.* **2020**, *10*, 11048. [CrossRef]
51. Boyd, G.E.; Adamson, A.W.; Myers, L.S. The exchange adsorption of ions from aqueous solutions by organic zeolites. II. Kinetics. *J. Am. Chem. Soc.* **1947**, *69*, 2836–2848. [CrossRef]
52. Yuh-Shan, H. Citation review of Lagergren kinetic rate equation on adsorption reactions. *Scientometrics* **2004**, *59*, 171–177. [CrossRef]
53. Goswami, M.; Borah, L.; Mahanta, D.; Phukan, P. Equilibrium modeling, kinetic and thermodynamic studies on the adsorption of Cr(VI) using activated carbon derived from matured tea leaves. *J. Porous Mater.* **2014**, *21*, 1025–1034. [CrossRef]